Article

A Comparative Study of the Catalytic Mechanisms of the Zinc and Cadmium Containing Carbonic Anhydrase

Tiziana Marino, Nino Russo, and Marirosa Toscano

J. Am. Chem. Soc., **2005**, 127 (12), 4242-4253• DOI: 10.1021/ja045546q • Publication Date (Web): 01 March 2005

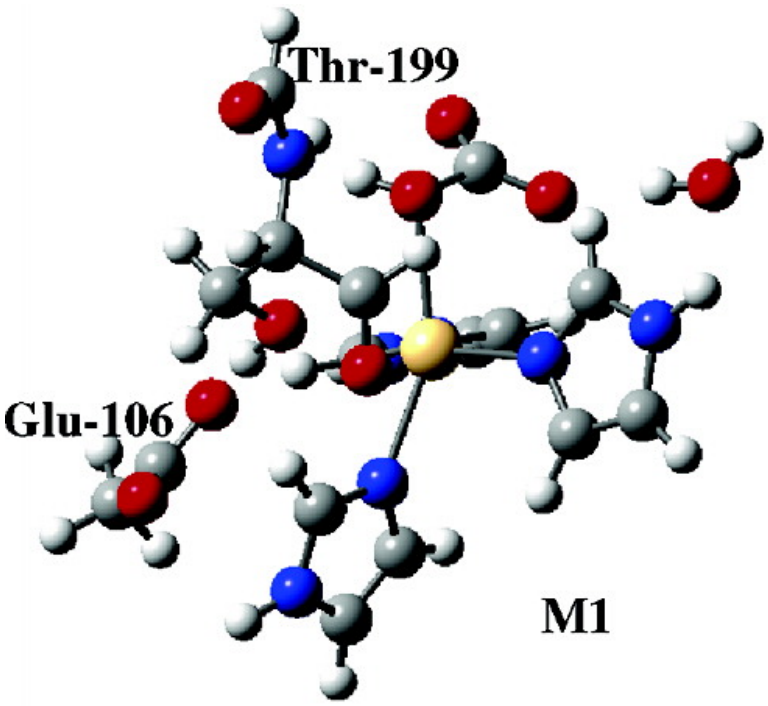

J|A|C|S
ARTICLES
Published on Web 03/01/2005

A Comparative Study of the Catalytic Mechanisms of the Zinc and Cadmium Containing Carbonic Anhydrase

Tiziana Marino, Nino Russo,* and Marirosa Toscano

Contribution from the Dipartimento di Chimica and Centro di Calcolo ad Alte Prestazioni per Elaborazioni Parallele e Distribuite-Centro d'Eccellenza MIUR, Università della Calabria, I-87030 Arcavacata di Rende (CS), Italy

Received July 24, 2004; E-mail: nrusso@unical.it

Abstract: The catalytic mechanism for the conversion of carbon dioxide to hydrogen carbonate by a cadmium containing carbonic anhydrase was explored at density functional level employing two different models to simulate the active center of the enzyme. In the first model, the histidine residues around the metal ion were replaced with imidazole groups. Instead, in the second one, the simplest model was extended introducing two amino acidic residues generally present in the neighbor of enzyme and a deep water molecule. The results showed that cadmium carbonic anhydrase follows a reaction mechanism that is favored thermodynamically but not kinetically with respect to that of the most usual zinc-containing enzyme, both in a vacuum and in a protein environment.

Introduction

Carbonic anhydrases (CA) are ubiquitous enzymes found in all animals and photosynthesizing organisms as well as in some nonphotosynthetic bacteria. They catalyze the reversible hydration of carbon dioxide: $CO_2 + H_2O \leftrightarrow HCO_3^- + H^+$.[1−6] The active site of the enzymes contains a zinc ion that is essential for catalysis.[7] Human carbonic anhydrase II (HCA II) is the most efficient enzyme with a turnover number of 10^6 s^{-1} at pH = 9 and 25 °C.[8,9]

The Zn^{2+} in CA can be replaced with other divalent metal ions such as Co^{2+}, Mn^{2+}, Ni^{2+}, Hg^{2+}, Cd^{2+}, and Cu^{2+}.[10−20] The substitution of the metal center occurs also in other enzymes. For instance, in the carboxypeptidase A, the Zn^{2+} can be replaced with Cd^{2+}: Cd-substituted enzyme continues to show esterase activity, but the peptidase activity is largely lost.[21] Mainly, the substitution in CA of the native zinc with another metal similar to that mentioned before[10−19] is used to gain more insight into the structure of Zn-CA. In fact, some of these metals is recognized as a powerful spectroscopic probe in biological systems.[13,22−26] The Co^{2+}- and Mn^{2+}-containing enzymes have shown substantial esterase and CO_2 hydration activity.[27,28] As verified in the work of Bauer et al.,[20] the Cd^{2+} enzyme also produces activities but at a higher pH value as compared to the Zn^{2+} derivatives. In the same work, performed by gel-filtration techniques,[20] it was carried out that the Cd^{2+} binds to the apoenzyme of CA more strongly than the Zn^{2+}. Moreover, the Cd^{2+} shows to have only one binding place in the enzyme which is identical with the Zn^{2+} one.[20] In another work,[29] the whole conformation of the Cd^{2+} enzyme was found to be the same as that of the Zn^{2+} enzyme.

Evidence of in vivo utilization of Cd^{2+} in CA was published by Price and Morel[30] and Morel et al.[31] CA constitutes a major use of Zn^{2+} in at least some marine *diatoms*. At the concentrations of trace metals found in the surface waters of the open ocean, inorganic carbon utilization by *Thalassiosira weissflogii*, a neritic species, was shown to be impaired.[31] Only in the year 2000, Lane and Morel[32] arrived at the surprising identification

(1) Bertini, I.; Luchinat, C. In *Bioinorganic Chemistry*; Bertini, I., Gray, H. B., Lippard, S. J., Valentine, J., Eds.; University Science Books: Mill Valley, CA, 1994.
(2) Botre, F., Gors, G., Storey, B. T., Eds. *Carbonic Anhydrase*; VCH: New York, 1991.
(3) Christianson, D. W. *Adv. Protein Chem.* **1991**, *42*, 281.
(4) Slverman, D. N.; Lindskog, S. *Acc. Chem. Res.* **1988**, *21*, 30.
(5) Dodgson, S. J., Tashian, R. E., Gros, G., Carter, N. D., Eds.; *The Carbonic Anhydrase*; Plenum Publishing Corporation: 1991.
(6) Lindskog, S. *Pharmacol. Ther.* **1997**, *74*, 1.
(7) Coleman, J. *Curr. Opin. Chem. Biol.* **1998**, *2*, 222.
(8) Khalifah, R. G. *J. Biol. Chem.* **1971,** *246*, 2561.
(9) Steiner, H.; Jonsson, B. H.; Lindskog, S. *Eur. J. Biochem.* **1975**, *59*, 253.
(10) Woolley, P. *Nature* **1975**, *258*, 677.
(11) Tu, C. K.; Silverman, D. N. *Biochemistry* **19**85, *24*, 5881.
(12) Wilkins, R. G.; Williams, K. R. *J. Am. Chem. Soc.* **1974**, *96*, 2241.
(13) Bertini, I.; Luchinat, C.; Monnani, R.; Roelens, S.; Moratal, J. M. *J. Am. Chem. Soc.* **1987**, *109*, 7855.
(14) Lanir, A.; Navon, G. *Biochemistry* **1972**, *11*, 3536.
(15) Led, J. J.; Neesgaard, E. *Biochemistry* **1987**, *26*, 183.
(16) Coleman, J. E. *J. Biol. Chem.* **1967**, *242*, 5212.
(17) Vallee, B. L., Gades, A. *Adv. Enzymol.* **1984**, *56*, 283.
(18) Coleman, J. E. *Nature* **1967**, *214*, 193.
(19) Lipscomb, W. N. *Annu. Rev. Biochem.* **1983**, *52*, 17.
(20) (a)Bauer, R.; Limkilde, P.; Johansen, J. T. *Biochemistry*, **1976**, *15*, 334. (b)Garmer, D. R.; Krauss, M. *J. Am. Chem. Soc.* **1992**, *114*, 6487. (c) Solà, Mestres, J.; Duran, M.; Carbo, R. *J. Chem. Inf. Comput. Sci.* **1994**, *34*, 1047.
(21) Coleman, J. E.; Vallee, B. L. *J. Biol. Chem.* **1961**, *236*, 2244.
(22) Bertini, I.; Canti, G.; Luchinat, C.; Scozzafava, A. *J. Am. Chem. Soc.* **1978**, *100*, 4873.
(23) Tu, C. K.; Silverman, D. N. *J. Am. Chem. Soc.* **1986**, *108*, 6065.
(24) Williams, T. K.; Henkens, R. W. *Biochemistry* **1985**, *24*, 2459.
(25) Haffner, P. H.; Coleman, J. E. *J. Biol. Chem.* **1975**, *14*, 681.
(26) Pesando, J. M. *Biochemistry* **1985**, *24*, 5881.
(27) Lindskog, S.; Henderson, L. E.; Kannan, K. K.; Liljas, A.; Nyman, P. O.; Strandberg, B. *Enzymes*, 3rd ed.; 1971; Vol. 5, p 587.
(28) Lanir, A.; Gradstajn, S.; Navon, G. *Biochemistry* **1975**, *14*, 242.
(29) Zavodsky, P.; Johansen, J. T.; Hvidt, A. *Eur. J. Biochem.* **1975**, *56*, 67.
(30) Price N. M.; Morel F. M. M. *Nature* **1990**, *344*, 658.
(31) Morel F. M. M.; Reinfelder, J. R.; Roberts S. B.; Chamberlain C. P.; Lee J. G.; Yee, D. *Nature* **1994**, *369*, 740.
(32) Lane, T. W.; Morel, F. M. M. *Proc. Natl. Acad. Sci. U.S.A.* **2000**, *97*, 4627.

10.1021/ja045546q CCC: $30.25

of the first special cadmium carbonic anhydrase (Cd-CA) synthesized by the same marine diatom under conditions where the zinc concentration was low.[27,28,33−35]

Many experimental[36−50] and theoretical[51−70] investigations on the mechanism of catalytic CO_2 hydration and on the coordination chemistry of zinc ion hydroxide (Zn−OH) exist in literature. In the greater portion of these studies, the authors use the simple $[(NH_3)_3Zn-OH]^+$ model catalyst to mimic the active center of the Zn-CA. Recent works[65,70] have suggested that a model in which the imidazole rings substitute the NH_3 molecules simulates better the enzyme active site enhancing the hydroxide nucleophilicity hence causing a lowering of the energetic barriers in the catalytic cycle. Finally, an advanced model for the Zn-CA site was proposed by Bottoni et al.[70] It includes, in the immediate proximity, the Zn−OH fragment, two amino acidic residues, Thr199 and Glu106, and a deep water molecule.

Several mechanisms were explored over the years to explain how the Zn-CA works. We summarize their most general aspects with the aid of Scheme 1.

Following the suggestions of Davis,[71] Coleman,[16] and Silverman and Lindskog,[4] Mertz et al.[52] proposed a catalytic process in which, after the deprotonation of the Zn-bound water molecule, the Zn−OH moiety (I of the Scheme 1), on nucleophilic attack to the free CO_2, generated the zinc-bound hydrogencarbonate ion (Lindskog intermediate, III in Scheme 1). The energetic barrier for the deprotonation process, corresponding to the energetic difference between the transition state II of the Scheme 1 and the separated reactants, was computed to be 13.1 kcal/mol at the AM1 level.[52]

Scheme 1

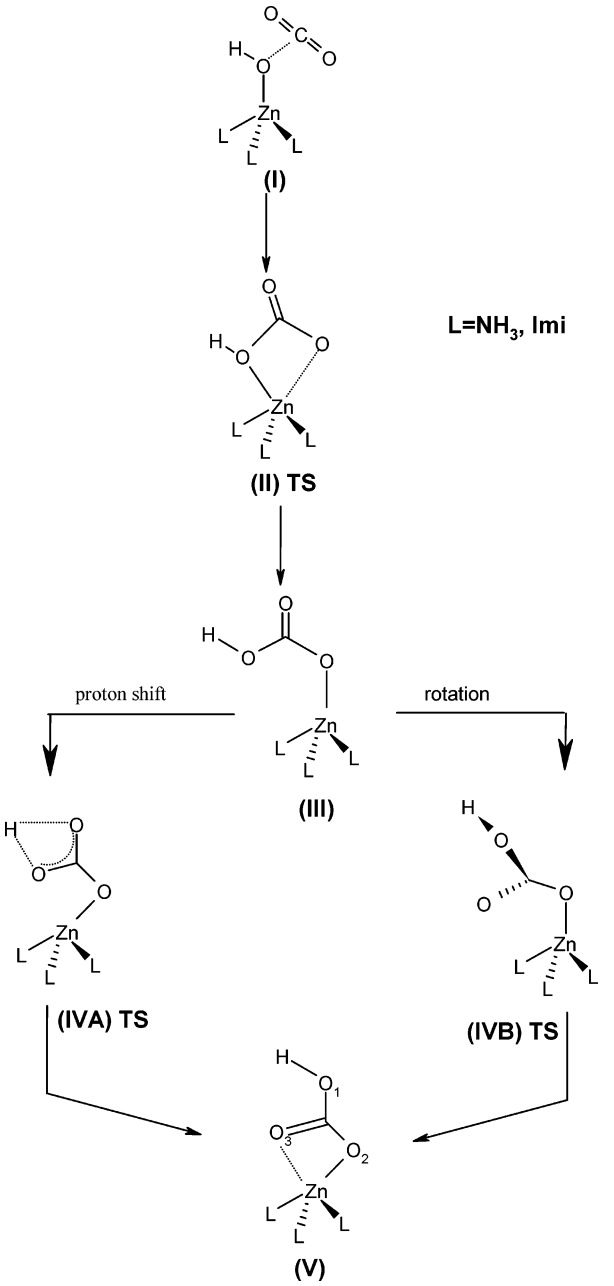

For the stabilization of $Zn-HCO_3^-$ species (III), two different ways were proposed. The former, known as the Lipskomb mechanism,[19] hypothesizes a proton transfer between the zinc-bound oxygen and another oxygen of the HCO_3^- group. The latter one, the so-called Lindskog mechanism,[72] suggests an internal rotation that causes the change of the oxygen atom

(33) Strasdeit, H. *Angew. Chem., Int. Ed.* **2001**, *40*, 707.
(34) Cullen, J. T.; Lane, T. W.; Morel, F. M. M.; Sherrel, R. M. *Nature* **1999**, *402*, 165.
(35) Lee J. G.; Morel F. M. M. *Mar. Ecol.: Prog. Ser.* **1995**, *127*, 305.
(36) Bertini, I.; Luchinat, C. *Acc. Chem. Res.* **1983**, *16*, 272.
(37) Silverman, D. N.; Lindskog, S. *Acc. Chem. Res.* **1988**, *21*, 30.
(38) Christianson, D. W.; Fierke, C. A. *Acc. Chem. Res.* **1996**, *29*, 331 and references therein.
(39) Woolley, P. *Nature* **1975**, *258*, 677.
(40) Liljas, A.; Kannan, K. K.; Bergsten, P. C.; Waara, I.; Friborg, K.; Strandberg, B.; Carlbom, U.; Jarup, L.; Lovgren, S.; Petef, M. *Nat. New Biol.* **1972**, *235*, 131.
(41) Eriksson, E. A., Jones, T. A.; Liljas, A. In *Zinc Enzymes*; Bertini, I., Luchinat, C., Maret, W., Zappezauer, M., Eds.; Birkhauser: Boston, 1986; Vol. 1, p 317.
(42) Hakansson, K.; Carlsson, M.; Svensson, L. A.; Liljas, A. *J. Mol. Biol.* **1992**, *227*, 1192.
(43) Kimura, E. *Acc. Chem. Res.* **2001**, *34*, 171 and references therein.
(44) Huang, C.; Lesburg, C. A.; Kiefer, L. L.; Fierke, C. A.; Christianson, D. W. *Biochemistry* **1996**, *35*, 3439.
(45) Lesburg, C. A.; Huang, C.; Christianson, D. W.; Fierke, C. A. *Biochemistry* **1997**, *36*, 15780.
(46) Zhang, X.; Hubbard, C. D.; van Eldik, R. *J. Phys. Chem.* **1996**, *100*, 9161.
(47) Nair, S. K.; Calderone, T. L.; Christianson, D. W.; Fierke, C. A. *J. Biol. Chem.* **1991**, *266*, 17320.
(48) Tu, C.; Tripp, B. C.; Ferry, J. G.; Silverman, D. N. *J. Am. Chem. Soc.* **2001**, *123*, 5861.
(49) Thoms, S. *J. Theor. Biol.* **2002**, *215*, 399.
(50) Schroder, D.; Schwartz, H.; Schenk, S.; Anders, E. *Angew. Chem., Int. Ed.* **2003**, *42*, 5087.
(51) (a) Liang, J.-Y.; Lipscomb, W. N. *J. Am. Chem. Soc.* **1986**, *108*, 5053. (b) Liang, J.-Y.; Lipscomb, W. N. *Biochemistry* **1987**, *26*, 5293.
(52) Merz, K. M.; Hoffmann, R.; Dewar, M. J. S. *J. Am. Chem. Soc.* **1989**, *111*, 5636.
(53) Liang, J.-Y.; Lipscomb, W. N. *Int. J. Quantum Chem.* **1989**, *36*, 299.
(54) Jacob, O.; Cardenas, R.; Tapia, O. *J. Am. Chem. Soc.* **1990**, *112*, 8692.
(55) Krauss, M.; Garmer, D. R. *J. Am. Chem. Soc.* **1991**, *113*, 6426.
(56) Zheng, Y.-J.; Merz, K. M. *J. Am. Chem. Soc.* **1992**, *114*, 10498.
(57) Sola, M.; Lledos, A.; Duran, M.; Bertran, J. *J. Am. Chem. Soc.* **1992**, *114*, 869.
(58) Sakurai, M.; Furuki, T.; Inoue, Y. *J. Phys. Chem.* **1995**, *99*, 17789.
(59) Murcko, M. A. *Theor. Chem. Acc.* **1997**, *96*, 56.
(60) Merz, K. M.; Banci, L. *J. Am. Chem. Soc.* **1997**, *119*, 863.
(61) Lu, D.; Voth, G. A. *J. Am. Chem. Soc.* **1998**, *120*, 4006.
(62) Toba, S.; Colombo, G.; Merz, K. M. *J. Am. Chem. Soc.* **1999**, *121*, 2290.
(63) Denisov, V. P.; Jonsson, B.-H.; Halle, B. *J. Am. Chem. Soc.* **1999**, *121*, 2327.
(64) Mauksch, M.; Brauer, M.; Weston, J.; Anders, E. *ChemBioChem* **2001**, *2*, 190.
(65) Brauer, M.; Perez-Lustres, J. L.; Weston, J.; Anders, E. *Inorg. Chem.* **2002**, *41*, 1454.
(66) Smedarchina, Z.; Siebrand, W.; Fernandez-Ramos, A.; Cui, Q. *J. Am. Chem. Soc.* **2003**, *125*, 243.
(67) Garmer, D. R. *J. Phys. Chem. B* **1997**, *101*, 2945.
(68) Cui, Q.; Karplus, M. *J. Phys. Chem. B* **2003**, *107*, 1071.
(69) Muguruma, C. J. *THEOCHEM* **1999**, *461*−*462*, 439.
(70) Bottoni, A.; Lanza, C. Z.; Miscione, G. P.; Spinelli, D. *J. Am. Chem. Soc.* **2004**, *126*, 1542.
(71) Davis, R. P. *J. Am. Chem. Soc.* **1959**, *81*, 5674.
(72) Lindskog, S. In *Zinc Enzymes*; Spiro, T. G., Ed.; Wiley: New York, 1983; p 77.

directly linked to the Zn ion. Many theoretical studies have allowed to compute the energetic barriers for the two possible rearrangements of Lindskog intermediate.[53,56,64,65,69] However, irrespective of the followed mechanism, the reaction product should be a permutational isomer (Lipscomb intermediate, V in Scheme 1) more stable than the Lindskog intermediate III.

The resulting zinc-coordinated HCO_3^- ion is then displaced from the metal ion by another water molecule which will be again deprotonated to regenerate the active catalyst.

All the involved species in the Scheme 1 were in turn the object of discussion.

Thoms,[49] on the basis of X-ray structure of the hydrogen-bond network in the catalytic site, suggested that the starting point of the cycle, i.e., the nucleophilic attack on CO_2, is the work of the zinc-bound water molecule rather than of the corresponding zinc-hydroxide (I). The formation of a certain number of hydrogen bonds was retained responsible for the stabilization of the transition state (II) by which the bond between the carbon atom of CO_2 and the oxygen atom linked to the metal center is established. With the study of Thoms[49] brings out the significant role of the amino acidic residues Thr199 and Glu106 in the surrounding medium. These residues, and no more the imidazole ring of the His64 as previously suggested,[4,52,68] were proposed as acceptors of the proton released by the zinc-bound water molecule. The relay function of Thr199 and Glu106, which can be carried out also by one or more water molecules, was suggested by Bertran et al.,[57] Bottoni et al.,[70] Muguruma[69] and Cui, and Karplus[68] to occur in some other step of the catalytic cycle like the bicarbonate rearrangement (IVa).

The discussion about the Lindskog intermediate (III) concerned both the coordination type of Zn^{2+} and its stability with respect to the Lipscomb one (V).

Brauer et al. [65] and Kimblin et al.[73] indicated for the Zn^{2+} ion a tetracoordinated complex, whereas Bottoni et al.[70] suggested a pentacoordinated intermediate. However, the discrepancies between these results can be ascribed to the different models used to simulate the active site of CA enzyme.

A more general agreement exists,[54−56,60,64,65,69,70] instead, on the major stability of the Lipscomb intermediate (V) with respect to that of Lindskog (III) except for the findings of Zeng and Mertz[56] that, in their MP2 study, define the Lindskog species as a "sink" in the whole mechanism, since its energy was computed to be 9.3 kcal/mol lower than that of the Lipscomb product.

Much less attention was devoted to the Cd−CA system.[32−35,74] Recently, a novel binuclear cadmium hydroxide complex was isolated and structurally and spectroscopically characterized that reacts with CO_2 to yield a binuclear cadmium carbonate complex.[75]

In the present investigation, we have undertaken a study on the activation mechanism of the CO_2 by Cd-CA at density functional level, by using two hybrid exchange correlation functionals and different basis sets. The nucleophilic attack on CO_2 was provided by cadmium-bound hydroxide and not by cadmium-bound water, as suggested by Thoms[49] in his study on the catalytic mechanism of human carbonic anhydrase.

Scheme 2

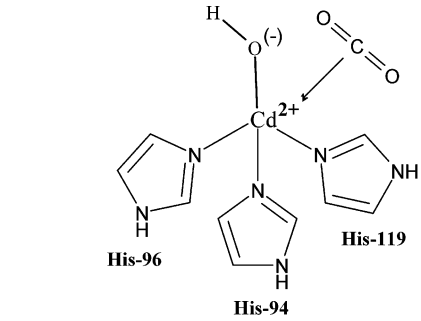

Model A

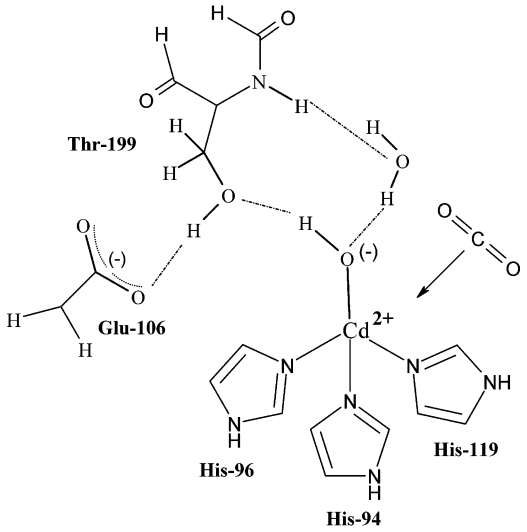

Model B

In particular, we have focused our attention on the internal rearrangements occurring after the attack on CO_2 to give the hydrogen carbonate ion.

With the aim to obtain information on the effect of the metal substitution on the structural and electronic properties of carbonic anhydrase, we have also studied the reaction path of the Zn-CA. Because of the presence in the literature of a previous theoretical investigation on this last system,[70] our study, performed at the same level of theory, was limited to the determination of the missing comparison data.

Finally, solvent effects were taken into account for a more reliable comparison with experimental observation concerning the different activities of the two enzymes.

Computational Details

Two distinct models, namely model A and model B depicted in the Scheme 2, were employed to simulate the Cd-CA active site.

The model A includes the Cd^{2+} cation linked to an −OH group, three imidazole rings belonging to the three histidine residues His94, His96, and His119, and a CO_2 molecule. The model system B was built up in the same manner proposed in the previous study concerning the Zn^{2+}-carbonic anhydrase mechanism.[70] It consists of all species present in the model A with the addition of two amino acidic residues, Glu106 and Thr199, the first of which is replaced with an acetate fragment to reduce the computational efforts and a water molecule (deep water).

(73) Kimblin, C.; Murphy, V. J.; Hascall, T.; Bridgewater, B. M.; Bonanno, J. B.; Parkin, G. *Inorg. Chem.* **2000**, *39*, 967.
(74) Allred, R. A.; Lenore, McAlexander, L. H.; Arif, A. M.; Berreau, L. M. *Inorg. Chem.* **2002**, *41*, 6790.
(75) Allred, R. A.; Arif, A. M.; Berreau, L. M. *J. Chem. Soc., Dalton Trans.* **2002**, 300.

All computations in the current investigation were performed at the density functional (DF) level with the Gaussian 03[76] package.

The Becke hybrid (B3) exchange and the Lee−Yang−Parr (LYP) correlation functionals[77] were chosen because, despite outdated, they were proven to be quite accurate in the description of enzymatic mechanisms.[78] In addition, since one of our purposes is the comparison with the recent B3LYP theoretical studies[64,65,70] concerning the Zn−CA system, our choice was practically forced.

However, computations on model B were redone with the modified Perdew and Wang exchange [79] and Becke 95 correlation[80] (MPWB1K) potential, recently proposed by Zao and Truhlar[81] as a suitable tool for obtaining a good description of hydrogen bonds and van der Waals type interactions.

The nature of stationary points was confirmed by vibrational analysis.

In the simplest model (model A), the relativistic compact effective potential (LANL2DZ)[82−84] for zinc and cadmium cations, and the standard all-electron valence double-ζ polarized basis set (6-31G*) for all other atoms, were used to fully/partially optimize all the encountered species.

As in the previous work on Zn-CA,[70] the system simulated by the model B was partitioned into two different regions that we treated at different accuracy levels. The region containing the atoms directly involved in the catalytic reaction was described by the DZVP[85] basis set. All other atoms (i.e., those belonging to the imidazole rings and involved in the M^{2+}−N bonds) were kept frozen during the geometry optimization and described by the less extended STO-3G basis set. For a more accurate estimate of the reaction energetics, DZVP single-point computations were carried out on B3LYP and MPWB1K optimized geometries.

Natural bond orbital (NBO)[86] analysis was used to calculate changes in the atomic charges along the reaction paths and to describe the nature of the metal ion−carbon dioxide bond.

Solvent effects were computed in the framework of a self-consistent reaction field polarized continuum model (SCRF-PCM)[87−89] using the UAHF[90] set of solvation radii to build the cavity for the solute in the gas-phase B3LYP and MPWB1K equilibrium geometries. The dielectric constant $\epsilon = 4$ was chosen on the basis of literature suggestions[78,91] that indicate this value as the most suitable one for the protein environment of the active site.

Scheme 3

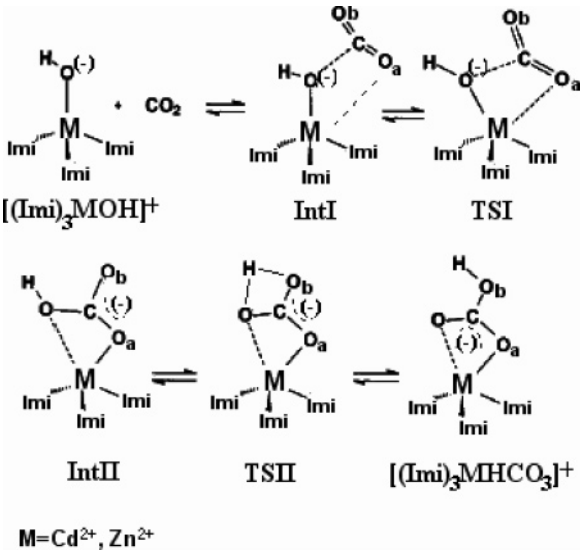

Results and Discussion

Model A. The species involved in the CA catalytic cycle and the labeling of all atoms are reported in Scheme 3. Equilibrium and transition state geometrical parameters for M^{2+}-CA (M = Cd, Zn) are collected in Table 1. The charge values of the atoms directly involved in the reaction, obtained from NBO analysis, are listed in Table 2. Figure 1 shows the energy profiles for both Zn- and Cd-CA derived from a partial optimization (imidazole rings and M^{2+}−N distances were kept frozen) of the molecular system simulating the active site of the enzyme.

The full optimization for the same system showed that energetic and structural data obtained using the two different procedures are comparable (see Supporting Information). Thus, at least in this particular case, the doubts raised by Bottoni et al.[70] about the opportunity to perform a complete optimization without altering the number of degrees of freedom of the biosystem are not confirmed. However, for purposes of homogeneity with the discussion concerning the simulation with model B, we will comment, for model A, only on the set of data obtained under geometrical constraints.

The general shape of the path relative to Cd-CA system is quite different from that of Zn-CA as far as both the height of the energetic barriers and intermediate stabilities are concerned. Similar behavior can be observed, instead, after the nucleophilic attack has occurred (see Figure 1).

Starting from the separated reactants, the IntI intermediate is reached without an energy barrier for both metal cations, but it is more stabilized for Cd^{2+} rather than for Zn^{2+} (−10.71 kcal/mol vs −3.17 kcal/mol). The different coordination chemistries of the two metal ions are already evident from the comparison between Zn- and Cd-IntI geometrical features. In fact, the distance O- -C (see Scheme 2 and Table 1) in Cd-IntI is very short (1.445 Å vs 2.605 Å in Zn^{2+}-IntI), the Cd^{2+}−O and Cd^{2+}−O_a bond lengths are 2.447 and 2.231 Å, respectively. The O_a−

(76) Frisch, M. J.; Trucks, G. W.; Schlegel, H. B.; Scuseria, G. E.; Robb, M. A.; Cheeseman, J. R.; Montgomery, Jr., J. A.; Vreven, T.; Kudin, K. N.; Burant, J. C.; Millam, J. M.; Iyengar, S. S.; Tomasi, J.; Barone, V.; Mennucci, B.; Cossi, M.; Scalmani, G.; Rega, N.; Petersson, G. A.; Nakatsuji, H.; Hada, M.; Ehara, M.; Toyota, K.; Fukuda, R.; Hasegawa, J.; Ishida, M.; Nakajima, T.; Honda, Y.; Kitao, O.; Nakai, H.; Klene, M.; Li, X.; Knox, J. E.; Hratchian, H. P.; Cross, J. B.; Adamo, C.; Jaramillo, J.; Gomperts, R.; Stratmann, R. E.; Yazyev, O.; Austin, A. J.; Cammi, R.; Pomelli, C.; Ochterski, J. W.; Ayala, P. Y.; Morokuma, K.; Voth, G. A.; Salvador, P.; Dannenberg, J. J.; Zakrzewski, V. G.; Dapprich, S.; Daniels, A. D.; Strain, M. C.; Farkas, O.; Malick, D. K.; Rabuck, A. D.; Raghavachari, K.; Foresman, J. B.; Ortiz, J. V.; Cui, Q.; Baboul, A. G.; Clifford, S.; Cioslowski, J.; Stefanov, B. B.; Liu, G.; Liashenko, A.; Piskorz, P.; Komaromi, I.; Martin, R. L.; Fox, D. J.; Keith, T.; Al-Laham, M. A.; Peng, C. Y.; Nanayakkara, A.; Challacombe, M.; Gill, P. M. W.; Johnson, B.; Chen, W.; Wong, M. W.; Gonzalez, C.; Pople, J. A. *Gaussian 03*, revision A.1; Gaussian, Inc.: Pittsburgh, PA, 2003.
(77) Stevens P. J.; Devlin, F. J.; Chablowski C. F.; Frisch M. J. *J. Phys. Chem.* **1994**, *98*, 11623.
(78) Noodleman, L.; Lovell, T.; Han, W.-G.; Li, J.; Himo F. *Chem. Rev.* **2004**, *104*, 459−508 and references therein.
(79) Becke, A. D. *J. Chem. Phys.* **1997**, *107*, 8554.
(80) Adamo, C.; Barone, V. *J. Chem. Phys.* **1998**, *108*, 664.
(81) Zhao, Y.; Truhlar, D. G. *J. Phys. Chem. A* **2004**, *108*, 6908.
(82) Hay, P. J.; Wadt, W. R. *J. Chem. Phys.* **1985**, *82*, 270.
(83) Wadt, W. R.; Hay, P. J. *J. Chem. Phys.* **1985**, *82*, 284.
(84) Hay, P. J.; Wadt, W. R. *J. Chem. Phys.* **1985**, *82*, 299.
(85) (a) Andzelm, J.; Radzio, E.; Salahub, D. R. E. *J. Comput. Chem.* **1985**, *6*, 520. (b) Goudbout, N.; Salahub, D. R.; Andzelm, J.; Wimmer, E. *Can. J. Chem.* **1992**, *70*, 560.
(86) Glendening, E. D.; Reed, A. E.; Carpenter, J. E.; Weinhold, F. *NBO*, version 3.1.
(87) Miertos, S.; Scrocco, E.; Tomasi, J. *Chem. Phys.* **1981**, *55*, 117.
(88) Miertos, S.; Tomasi, J. *Chem. Phys.* **1982**, *65*, 239.
(89) Cossi, M.; Barone, V.; Commi, R.; Tomasi, J. *J. Chem. Phys.* **1996**, *255*, 327.
(90) Barone, V.; Cossi, M.; Menucci, B.; Tomasi, J. *J. Chem. Phys.* **1997**, *107*, 3210.
(91) Blomberg, M. R. A.; Siegbahn, P. E. M.; Babcock, G. T. *J. Am. Chem. Soc.* **1998**, *120*, 8812.

Table 1. Main Geometrical Parameters of the Intermediates and Transition States Encountered in the Cd- and Zn-CA Energy Profiles Using the Model A to Simulate the Active Site (Distances Are in Å and Valence Angles in Degrees)

	$[(Imi)_3CdOH]^+$	Cd-IntI	Cd-TS1	Cd-IntII	Cd-TS2	$[(Imi)_3CdHCO_3]+$
Cd^{2+}- -O	2.086	2.447	2.557	2.809	2.355	2.432
Cd^{2+}- -O_a		2.231	2.182	2.164	2.371	2.269
O- -C		1.445	1.436	1.435	1.362	1.270
C- -O_a		1.281	1.284	1.283	1.254	1.265
C- -O_b		1.210	1.211	1.213	1.279	1.349
O_b- -H					1.339	0.972
O- -H	0.967	0.972	0.972	0.973	1.239	
O_a- -C- -O_b		132.87	131.98	131.31	133.65	116.66
O- -C- -O_a		108.52	109.27	110.49	120.82	124.02
	$[(Imi)_3ZnOH]^+$	Zn-IntI	Zn-TS1	Zn-IntII	Zn-TS2	$[(Imi)_3ZnHCO_3]^+$
Zn^{2+}- -O	1.878	1.894	1.919	3.078	3.078	2.426
Zn^{2+}- -O_a			2.875	1.949	1.985	2.038
O- -C		2.605	1.801	1.418	1.333	1.261
C- -O_a		1.174	1.208	1.287	1.268	1.274
C- -O_b		1.168	1.190	1.214	1.283	1.347
O_b- -H					1.313	0.972
O- -H	0.966	0.966	0.959	0.973	1.266	
O_a- -C- -O_b		173.82	146.00	129.61	128.49	116.04
O- -C- -O_a		95.80	102.95	111.68	124.58	123.55

Table 2. Atomic Net Charges (in |e|) Obtained by the NBO Analysis for the Species Encountered in the Cd- and Zn-CA Energy Profiles Using the Model A to Simulate the Active Site

	Cd	Zn
	$[(Imi)_3MOH]^+$	
q_M	1.593	1.606
q_O	−1.246	−1.274
	IntI	
q_M	1.653	1.635
q_O	−0.871	−1.272
q_{Oa}	−0.892	−0.567
q_{Ob}	−0.655	−0.521
q_C	1.026	1.069
	TSI	
q_M	1.651	1.656
q_O	−0.858	−1.068
q_{Oa}	−0.902	−0.716
q_{Ob}	−0.657	−0.601
q_C	1.035	1.028
	IntII	
q_M	1.650	1.663
q_O	−0.848	−0.942
q_{Oa}	−0.902	−0.824
q_{Ob}	−0.661	−0.660
q_C	1.031	1.041
	TSII	
q_M	1.654	1.663
q_O	−0.909	−0.846
q_{Oa}	−0.818	−0.883
q_{Ob}	−0.712	−0.712
q_C	1.022	1.041
	$[(Imi)_3MHCO_3]^+$	
q_M	1.647	1.658
q_O	−0.856	−0.839
q_{Oa}	−0.840	−0.869
q_{Ob}	−0.711	−0.707
q_C	1.043	1.046

C−O_b valence angle measures 133°. The cadmium ion appears to be pentacoordinated.

Instead, in Zn-IntI, it can be observed that the geometrical parameters of each fragment do not differ appreciably from those of isolated units ($[(Imi)_3ZnOH]^+$ and CO_2) and the cation appears to be tetracoordinated. The CO_2 fragment retains a valence angle very close to 180° suggesting a scarce activation of carbon dioxide.

The higher coordination number of Cd^{2+} with respect to Zn^{2+} is easily ascribable to the larger size of the first cation. Besides the above-mentioned geometrical differences, other important remarks derive from NBO analysis.

In Cd-IntI, a strongly polarized σ bond is formed between O and C (with 71.63% participation of oxygen, $q_O = -0.871$ |e|, $q_C = 1.026$ |e|; see Table 2) in which a carbon orbital with approximate sp hybridization is involved. The oxygen atoms of the CO_2 fragment are differently charged ($q_{Oa} = -0.892$ |e| and $q_{Ob} = -0.655$ |e|) supporting the already happened nucleophilic attack.

In Zn-IntI NBO analysis, no trace of a σ bond between O and C is found, and atomic net charge values, very similar to those of free CO_2 molecule ($q_{Oa} = -0.567$ and $q_{Ob} = -0.521$ |e| vs $q_O = -0.543$ |e|), imply the formation of a van der Waals intermediate.

TSI (see Scheme 3) is the transition state connecting the two IntI and IntII intermediates.

Cd-TSI is structurally similar to Cd-IntI with the O−Cd^{2+} distance lengthened by 0.11 Å and the Oa−Cd^{2+} bond longer by only 0.04 Å (Table 1). This transition state lies at only 1.37 kcal/mol with respect to Cd-IntI according to the fact that they have comparable geometrical features. Moreover, as observed for Cd-IntI, NBO analysis reveals, also in Cd-TSI, a σ bond between the O and C atoms (their contributions to the molecular orbital are 71.32% and 28.68%, respectively). Charge values are $q_O = -0.858$ and $q_C = 1.035$ |e| (Table 2).

Zn-TSI lies at 4.29 kcal/mol above Zn-IntI. These two structures show significant differences mainly as far as the O- -C distance and the O_a−C−O_b valence angle are concerned. In fact, in TS1, the bond shortens by about 0.80 Å, and the angle fastens until 148.4° (Table 1). However, the metal center remains tetracoordinated as in Zn-IntI.

In IntII, the hydrogen carbonate is already formed. The most relevant aspect in Cd-IntII is the breaking of the O−Cd^{2+} bond that leaves the hydrogen carbonate fragment bound with cadmium ion in a monodentate fashion. The covalent bond between O and C centers, results from an orbital overlap in which carbon participates 28.93% ($q_C = 1.031$ |e|) and oxygen 71.07% ($q_O = -0.848$ e) (see Table 2). Cd-IntII is located at only 0.68 kcal/mol below TSI. This small energy difference accounts for the structural analogies among all IntI, TSI, and IntII species.

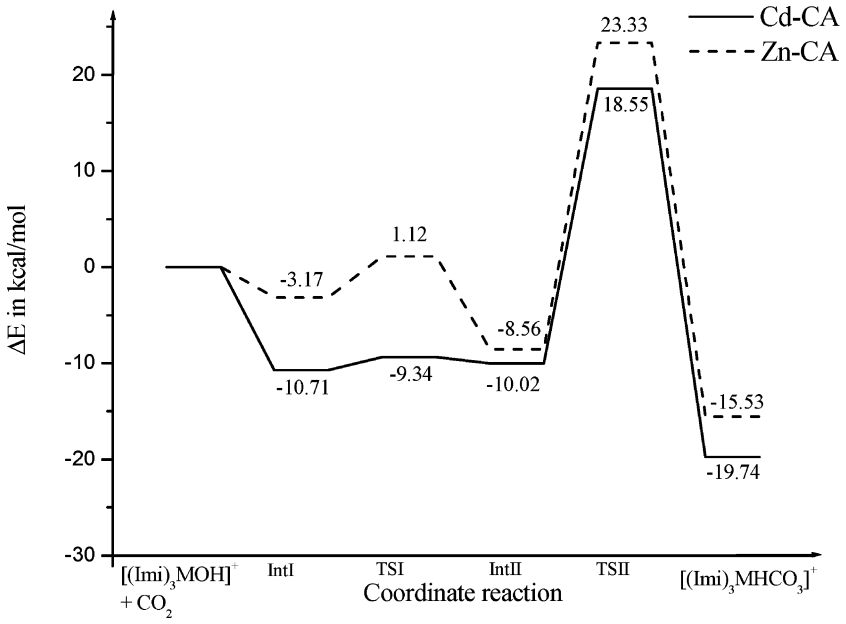

Figure 1. B3LYP/DZVP Potential energy profiles for the Zn- and Cd-CA obtained with partial optimization of the site active, in the simulation with model A.

Zn-IntII lies at 9.68 kcal/mol below Zn-TSI. The analysis of the geometrical parameters demonstrates how, at this level, it occurs at the greatest structural reorganization. The rearrangement carries out substantially through a clockwise rotation of the hydrogen carbonate fragment that induces the strengthening of the $Zn^{2+}-O_a$ (2.877 vs 1.949 Å) and the weakening of the $Zn^{2+}-O$ (1.920 vs 3.078 Å) bonds.

Cd-TSII and Zn-TSII are the transition state leading to the final products. Both lie at very high energy (28.57 and 31.89 kcal/mol above IntII for Cd^{2+} and Zn^{2+}, respectively) and suggest an intramolecular proton transfer between the O and O_b atoms. These transition states introduce the most convenient conditions for the leaving of the hydrogen carbonate group when a water molecule comes in to regenerate the active catalyst. In particular, the hydrogen shift between the two oxygen atoms O and O_b allows redistribution of single and double bonds in the HCO_3^- fragment in such a way that the $C-O_a$ length would be quite short to favor the displacement of the whole group. The conversion of IntII in the final product represents the rate-determining step in the reaction path for both metal centers.

The reaction appears more exothermic in the case of the cadmium ion. In particular, the energy value of the $[(Imi)_3CdHCO_3]^+$ species is about 4.0 kcal/mol lower than that of $[(Imi)_3ZnHCO_3]^+$.

On the basis of the obtained results, and contrary to what is experimentally[73,92,93] found, the Cd-CA enzyme shows an action mechanism more favorable with respect to that of Zn-CA: the reaction barriers are in general lower suggesting a more likely kinetic besides a better thermodynamic.

Model B. The symbols employed to indicate the Cd-CA intermediates and transition states obtained with the model B (see Scheme 2 and Figures 2 and 3) are the same as those used in the work of Bottoni et al.[70] concerning the Zn-CA system. The B3LYP/DZVP reaction profile is reported in Figure 4a, and the relative energies of stationary points along the path are collected in Table 3 together with data for Zn-CA.[70]

The nucleophilic attack of an −OH lone pair of M0 (naked enzyme) on the carbon atom of CO_2 gives rise to the intermediate M1 (see Figure 2) without an activation barrier. Contrary to what happens for Zn-CA, in which M1 is located at −6.03 kcal/mol, in the case of Cd-CA, this species appears strongly stabilized (it lies at −34.33 kcal/mol below M0 and CO_2 separated reactants whose energy was taken as reference). Like in the case of model A, the differences concerning the geometrical parameters around the two metal centers in M1 are remarkable.

The distance between O and C atoms (the labels of the atoms belonging to the active site are the same used for the model A) is, in the case of cadmium containing enzyme, much shorter than in the case of Zn−CA[70] (1.481 Å vs 2.630 Å, respectively). The cadmium ion appears tetracoordinated with the $Cd^{2+}-O$ and $Cd^{2+}-O_a$ bonds of 2.437 and 3.161 Å, respectively.

A charge transfer of about 0.41 |e|, from −OH group to CO_2 moiety (see Table 4), occurs during the nucleophilic attack as suggested by the NBO analysis (atomic net charge values on oxygen are −1.312 and −0.896 |e| before and after the attack, respectively). A σ bond between the O and C atom of CO_2 substrate is found. In this bond the carbon contributes 27.33%, and oxygen, 72.67%.

The hydrogen bond involving the Thr199 and Glu106 residues shortens on going from M0 to M1 (1.639 Å vs 1.543 Å).

In the case of the zinc enzyme, the Mulliken population analysis indicated the predominantly electrostatic nature of the interaction between the −OH and CO_2 groups.[70]

The activation energy required for the conversion M1 → M2 is considerably high (54.34 kcal/mol) in the case of Cd-CA. In TS1, the distance between the −OH group and the carbon atom of CO_2 is 1.476 Å (i.e., slightly shorter than in M1). The hydrogen carbonate fragment, lying on a plane different from that of the remaining molecular system, is practically monocoordinated to the Cd^{2+} ion ($Cd^{2+}-O$ = 2.239 Å), since the $Cd-O_a$ distance is still quite long (2.809 Å) for a bicoordination. The hydrogen bond network is arranged around the reaction

(92) Kimblin, C.; Parkin, G. *Inorg. Chem.* **1996**, *35*, 6912.
(93) Ejnik, J.; Munoz, A.; Gan, T.; Shaw, F. C., III; Petering, D. H. J. *JBIC* **1999**, *4*, 784.

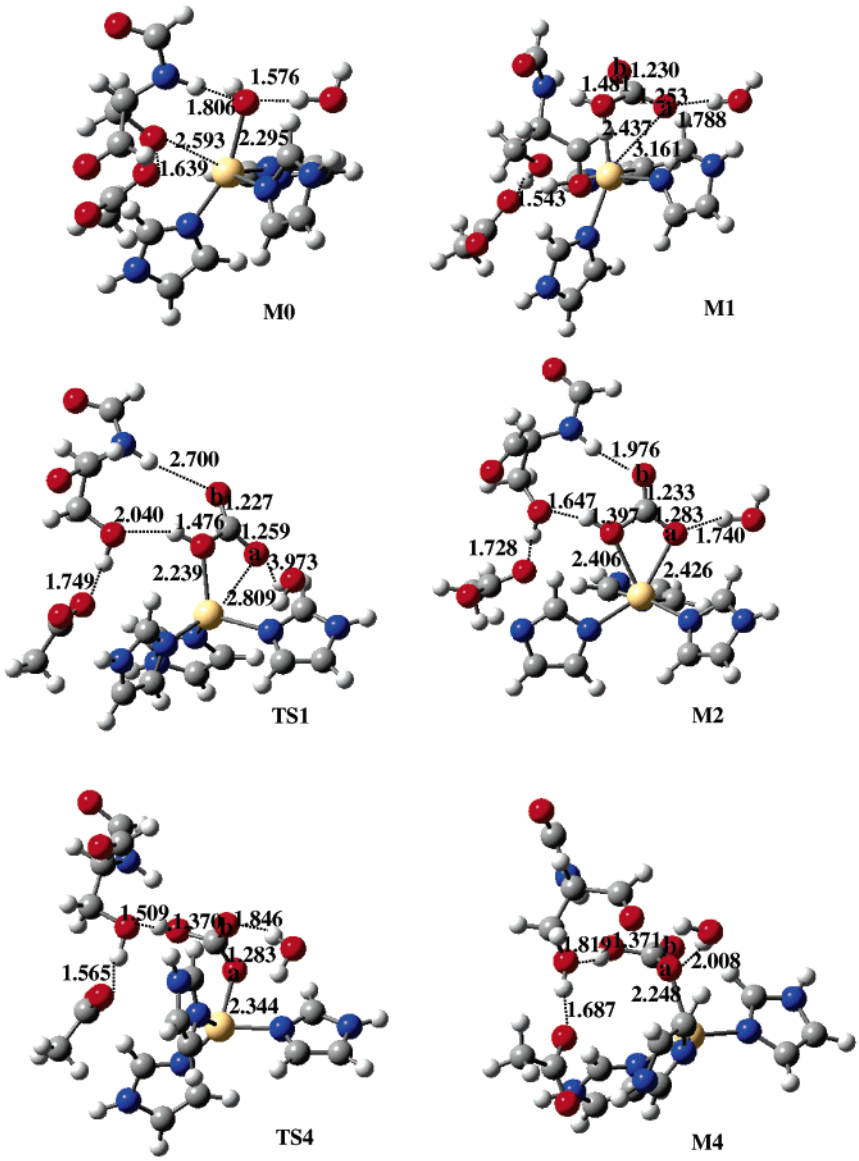

Figure 2. Equilibrium structures of intermediates and transition states along the Cd-CA reaction path (model B).

site differently than in M1. The water molecule locates between the CO_2 moiety and the metal center (see Figure 2). The new water disposition causes the breaking of its H-bond with O_a (3.973 vs 1.788 Å). The H-bond between −OH of Thr199 and the oxygen atom of the Glu106 residue lengthens becoming 1.749 Å (1.543 Å in M1). Two new H-interactions appear. The former, quite weak (2.700 Å), occurs between the −NH donor of Thr199 and the O_b atom of hydrogen carbonate. The latter one (2.040 Å), involves the −OH acceptor of Thr199 and the hydroxyl group of the hydrogen carbonate moiety.

For Zn−CA, TS1 is rashly defined as a barrier because of the small energy difference with respect to M1 (only 0.04 kcal/mol)[70](see Table 2). Bottoni et al.[70] explain this low barrier with the increase of hydrogen-bond interaction strength in the transformation M1 → TS1. This does not happen in Cd-CA, but it is worth noting that Cd-TS1 is substantially different from Zn-TS1. In fact, the imaginary vibrational frequency, in Cd-TS1, corresponds to the stretching mode of the incoming Cd^{2+}−O_a bond coupled to the out of plane HCO_3^- fragment that assumes a planar disposition with respect to the metal center. Instead, Zn-TS1 represents the transition state for the C−O bond formation.

The active site geometrical features of M2, obtained via TS1, are different from those of M1 (see Figure 2), and in addition, it is 27.31 kcal/mol lower in energy (see Table 3). The position of the deep water molecule remains almost the same: the H-bond with one of the oxygen atoms of the hydrogen carbonate fragment reduces by only 0.048 Å with respect to that in M1. The two new H-interactions involving Thr199 and the bicarbonate fragment, already present in TS1, appear to be reinforced (1.976 vs 2.700 Å and 1.647 vs 2.040 Å). The H-bond between Thr199 and Glu106 is now longer than that in M1 (1.728 vs 1.543 Å) (see Figure 2).

The charges distribution on the hydrogen carbonate fragment indicates a negative charge on the O_a atom major than in M1 (−0.927 |e| vs −0.850 |e|) and a charge on the oxygen O_b minor than in M1 (−0.767 |e| vs −0.792 |e|). The charge on all other atoms can be found in Table 4. At present, the Cd^{2+} ion is pentacoordinated. The tendency to the pentacoordination was already evident in TS1 where the Cd^{2+}−O_a bond is shorter than

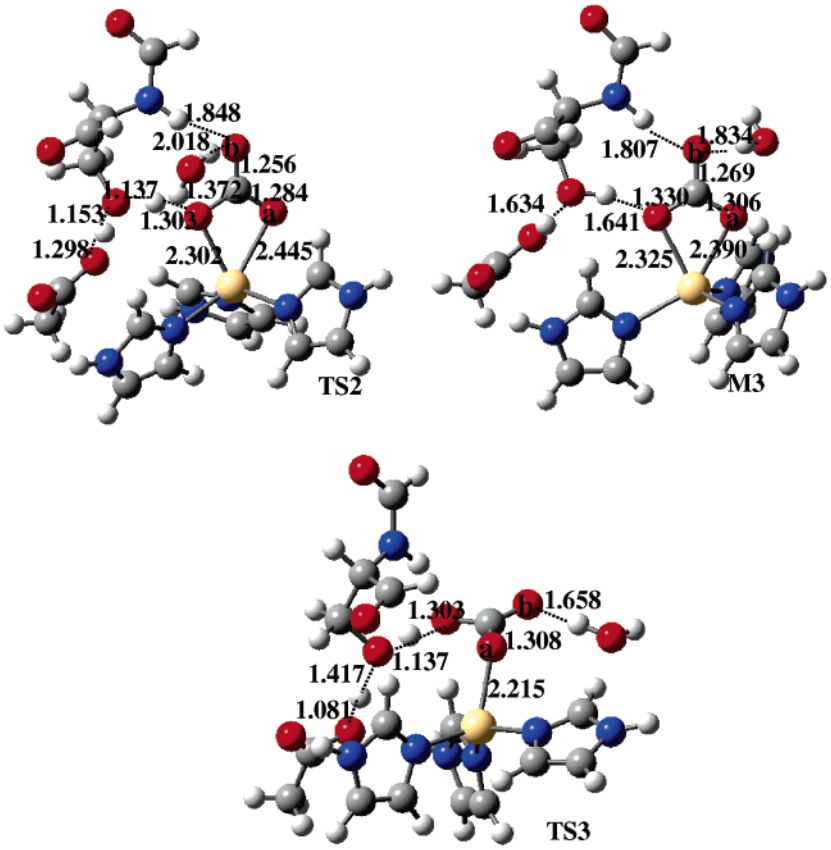

Figure 3. Equilibrium structures of intermediates and transition states along the Cd-CA reaction path (model B).

that in M1 to the point of becoming very similar to the $Cd^{2+}-O$ length in M2 (2.426 and 2.406 Å, respectively).

For Zn-CA, M2 lies at 12.16 kcal/mol below M1. The geometry reorganization leading to M2 determines a displacement of the water molecule that goes closer to the hydrogen carbonate fragment and a strengthening of two hydrogen bonds already existing in M1.[70] The zinc ion presents a five coordination.[70]

In the Cd-CA enzyme, M2 can be connected to the M4 intermediate, through two distinct reaction channels. The first, M2 → TS4 → M4, is a one-step process, whereas the second, M2 → TS2 → M3 and M3 → TS3 → M4, proceeds in two steps (see Figure 4a).

In the former channel, the M2 → M4 interconversion occurs through an internal rotation of the bicarbonate moiety around the $C-O_a$ bond, as suggested by the observation of the TS4 structural features. The rotation requires a very big amount of energy (about 77.94 kcal/mol). This is not surprising if we consider the stability of M2 species and the geometrical modifications that take place in going from M2 to TS4. The Figure 2 shows how the similarities between these two species are very few.

In TS4, only a hydrogen bond (of 1.509 Å) joins the amino acidic Thr199 and Glu106 region to the hydrogen carbonate fragment. The cadmium ion becomes tetracoordinated, since the $Cd^{2+}-O$ bond is broken and the hydrogen carbonate group remains anchored to Cd^{2+} through the O_a atom ($Cd^{2+}-O_a$ = 2.344 Å).

Imaginary vibrational frequency corresponds to the torsion of bicarbonate around the $C-O_a$ bond.

In M4, the Cd^{2+} ion is still linked to the O_a atom with a distance shorter (2.248 Å) than that in M2. Another difference with respect to TS4 concerns the length of the hydrogen bond between the Thr199 and Glu106 residues that becomes longer by 0.122 Å. The water molecule (see Figure 2), bound to the O_b atom in TS4, is now attached to the O_a atom (2.008 Å) like in M2. It is found in a suitable orientation to attack the cadmium ion that now presents a free coordination position, to restore the catalyst.

In the first step of the second reaction channel, the transition state TS2 connects the M2 and M3 intermediates. The conversion, occurring through two simultaneous proton transfers between threonine and glutamate and bicarbonate and threonine residues, requires 69.52 kcal/mol (see Figure 4a). The vibrational imaginary mode indicates clearly the switch of protons between the two amino acid residues and between bicarbonate and Thr199. The geometrical features of TS2 show a Cd^{2+} ion linked to the O_a and O atoms with distances of 2.445 and 2.302 Å, respectively. The water molecule forms a H-bond with the O_b oxygen of the bicarbonate fragment (2.018 Å) (see Figure 3) as a consequence of the negative charge increasing on this atom that is losing the proton.

The M3 intermediate lies at 27.40 kcal/mol above M2. In this species, the glutamate residue is protonated and the bicarbonate fragment has practically lost the proton giving rise to the CO_3^{2-} anion. The metal center appears to be still pentacoordinated (the $Cd^{2+}-O$ and $Cd^{2+}-O_a$ distances are of 2.325 and 2.390 Å, respectively). The deep water molecule is, like in the transition state TS2, involved in a hydrogen bond with the O_b atom (1.834 Å).

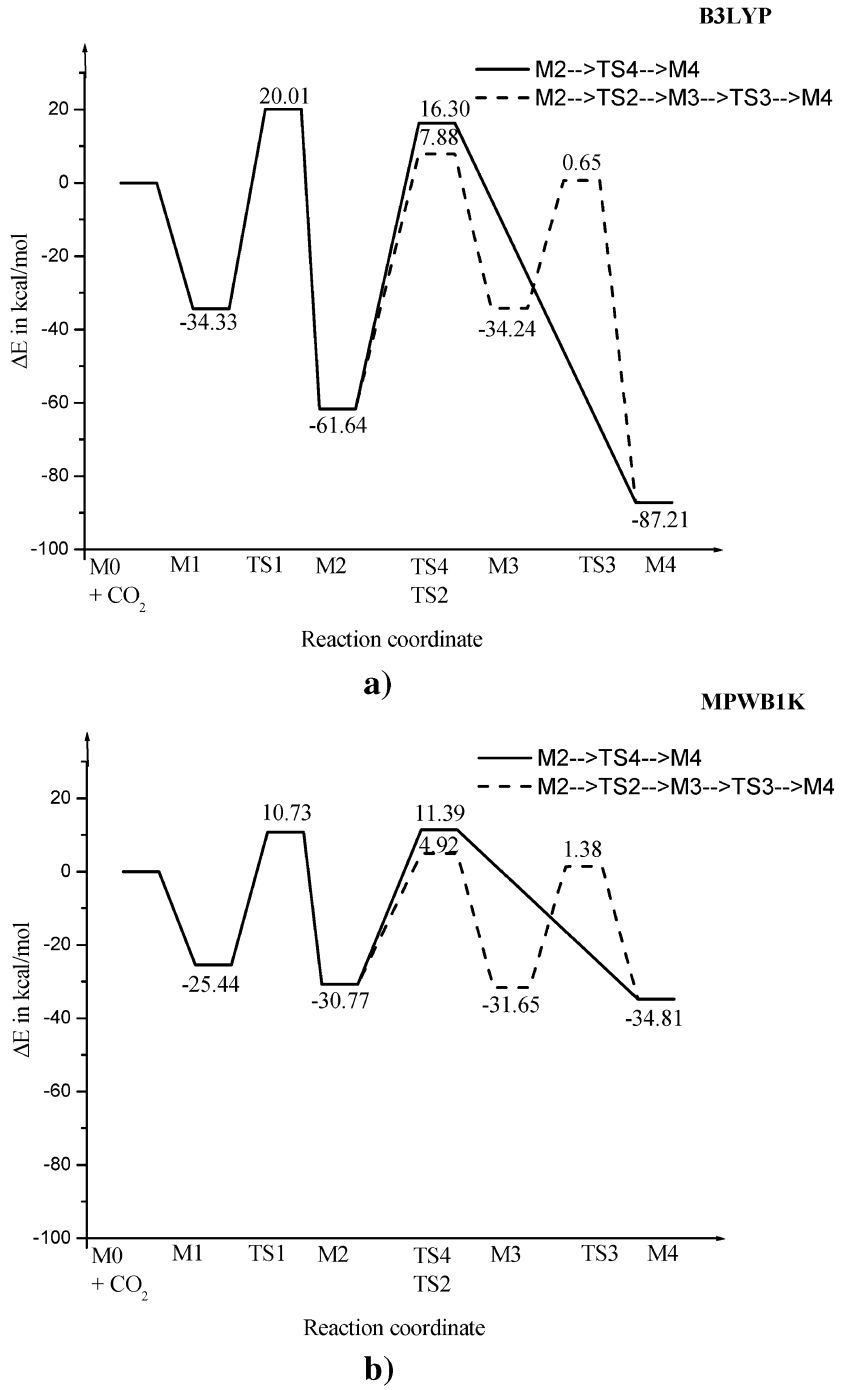

Figure 4. (a) B3LYP/DZVP and (b) MPWB1K/DZVP potential energy profiles for the Cd-CA (simulation with model B).

Starting from M3, a barrier of about 35 kcal/mol must be overcome to reach the final M4 complex. TS3 (see Figure 3) is a four-coordinated species where the $Cd^{2+}-O_a$ distance is shortening (2.215 Å) and the $Cd^{2+}-O$ bond is completely broken (4.109 Å). The rotation of the CO_3^{2-} group makes easier the proton transfer between the oxygen of the Thr199 residue and the O atom of the CO_3^{2-} moiety. Another proton transfer occurs between the residues Glu106 and Thr199 giving back a negatively charged glutamate. This double proton-transfer mechanism involving Thr199 and Glu106 is similar to the proton shuttle mechanism proposed to explain the deprotonation of the zinc -bound water enzyme.[52]

The product of the bicarbonate rearrangement (M4) is 42.97 kcal/mol more stable than M3.

Although also for Zn-CA two different reaction channels leading from M2 to M4 were hypothesized,[70] the results are significantly different from that obtained in the case of Cd-CA. The differences concern both the mutual stability of intermediates and the height of barriers. Contrary to the reaction path of zinc-containing enzyme,[70] that of cadmium is characterized by deep holes and high barriers; thus, despite the major exothermicity, the Cd-CA enzyme is prevented from carrying out its activity easily. This fact was already observed in the previous experimental studies on cadmium CA[73,92,93] that

Table 3. B3LYP Relative Energies (kcal/mol) Obtained with the DZVP Basis Set for Intermediates and Transition States of Cadmium Containing Carbonic Anhydrase Reaction Cycle for Model B (Simulation with Model B)

species	Cd DZVP	Zn[a] DZVP
M0	0.0	0.0
M1	−34.33	−6.03
TS1	20.01	−5.99
M2	−61.64	−18.19
TS4	16.30	3.20
M4	−87.21	−21.89
TS2	7.88	−15.81
M3	−34.24	−18.41
TS3	0.65	−6.20

[a] Reference 70.

Table 4. Atomic Net Charges (in |e|) Obtained by the NBO Analysis for the Species Encountered in the Cd-CA Energy Profiles Using the Model B to Simulate the Active Site

	M0	M4
q_{Cd}	1.260	1.202
q_{O}	−1.312	−1.015
q_{Oa}		−0.781
q_{Ob}		−0.810
q_{C}		1.125
	M1	**TS2**
q_{Cd}	1.189	1.285
q_{O}	−0.896	−1.035
q_{Oa}	−0.850	−0.925
q_{Ob}	−0.792	−0.835
q_{C}	1.105	1.131
	TS1	**M3**
q_{Cd}	1.259	1.232
q_{O}	−0.981	−1.017
q_{Oa}	−0.873	−0.993
q_{Ob}	−0.753	−0.865
q_{C}	1.117	1.130
	M2	**TS3**
q_{Cd}	1.237	1.255
q_{O}	−0.919	−1.033
q_{Oa}	−0.927	−0.818
q_{Ob}	−0.767	−0.906
q_{C}	1.131	1.133
		TS4
q_{Cd}		1.226
q_{O}		−0.846
q_{Oa}		−0.935
q_{Ob}		−0.848
q_{C}		1.113

attribute the different activity of cadmium and zinc enzymes to the different coordination chemistries of the metal ions that in turn depend on their size. In addition, they focus attention to the minor acid character of cadmium with respect to zinc.

The fact that the Cd^{2+} is weaker than Zn^{2+} as a Lewis acid and that it has a minor polarizing effect on its environment can decide if the fourth metal ion ligand, in the initial form of enzyme, can be present as an −OH group or a water molecule, but we have chosen to consider the same starting geometry for both enzymes, although we knew that the cadmium-hydroxide intermediate is generally present at more basic pH values. This means that, in our theoretical investigation, the minor acidity of the cadmium ion can have importance only as far as the strength with which the metal cation binds the CO_2 is concerned. In fact, the oxygen atom of the −OH group, in Cd−CA M0, has a charge more negative than that on the same atom in Zn-CA M0 (−1.312 vs −1.010 |e|, respectively), and thus it can establish with the substrate a stronger bond. This is confirmed by the NBO analysis and by the greater stability of all cadmium intermediates with respect to those of zinc along the whole reaction path.

Really, it is sufficient to stop at the intermediate M2 to understand that too large modifications in the geometry, and hence big amounts of energy, are necessary to continue the next transformations until M4. In the case of Zn-CA, the crucial steps are TS2 or TS4 depending if the transformation of M2 occurs through two proton shifts or a rotation. The same behavior can be observed in Cd-CA.

The coordination chemistry of the two cations plays an important role in determining the catalytic activity of the CA enzyme. Literature sources[1] indicate the ability of zinc to switch between four- and five-coordinate species without any appreciable barrier. This can be really observed in the Zn-CA catalytic mechanism,[70] unless other rearrangements that do not concern the coordination of Zn. On the contrary, cadmium does not show the same flexibility and the intermediates with different coordination are always separated by high interconversion barriers.

The model B overturns completely the results obtained with the small model A. Now, our findings are in agreement with the experimental observation[73,92,93] that indicates how Zn-CA be decidedly more active than Cd-CA (the activity of Cd-CA was estimated to be only 2% of that of Zn-CA).[94] This fact suggests that the role played by the amino acidic residues and by the deep water molecule is of fundamental importance in the active site simulation. These residues, as well as the deep water molecule, are involved in the formation of several hydrogen bonds and participate actively to the proton shifts that occur along the reaction path. Bottoni et al.,[70] in their work on Zn-CA, emphasize the same key role of Glu106 and Thr199. In fact, if we compare our results with those obtained by these authors, we find that the problems of the cadmium enzyme begin at the TS1 level, when, contrary to what occurs for the zinc enzyme, the excessive destabilization of this species, with respect to M1 intermediate, is caused by the disappearance or the weakening of the mentioned hydrogen bonds.

Computations on model B for Cd-CA were redone using the MPWB1K functional, and the new energetic profile was depicted in Figure 4b. From the comparison between the two B3LYP and MPWB1K paths, we can note that the second profile is flatter than the first one, since all the intermediates appear to be destabilized, whereas the transition states are stabilized.

On the basis of the MPWB1K description, the catalytic mechanism results kinetically easier.

The structural characters of the species along this last path are substantially the same as those obtained at the B3LYP level, except for the H-bond lengths that appear longer or shorter depending on the circumstances (Cartesian coordinates for both B3LYP and MPWB1K computations are provided as Supporting Information). Hence, the different energetics can be attributed

(94) Bertini, I.; Luchinat, C.; Viezzoli, M. S. In *Zinc Enzymes*; Bertini, I., Luchinat, C., Maret, W., Zeppezauer, M., Eds.; *Progress in Inorganic Biochemistry and Biophysics*, Vol. 1; Birkhauser: Boston, MA, 1986; Chapter 3.

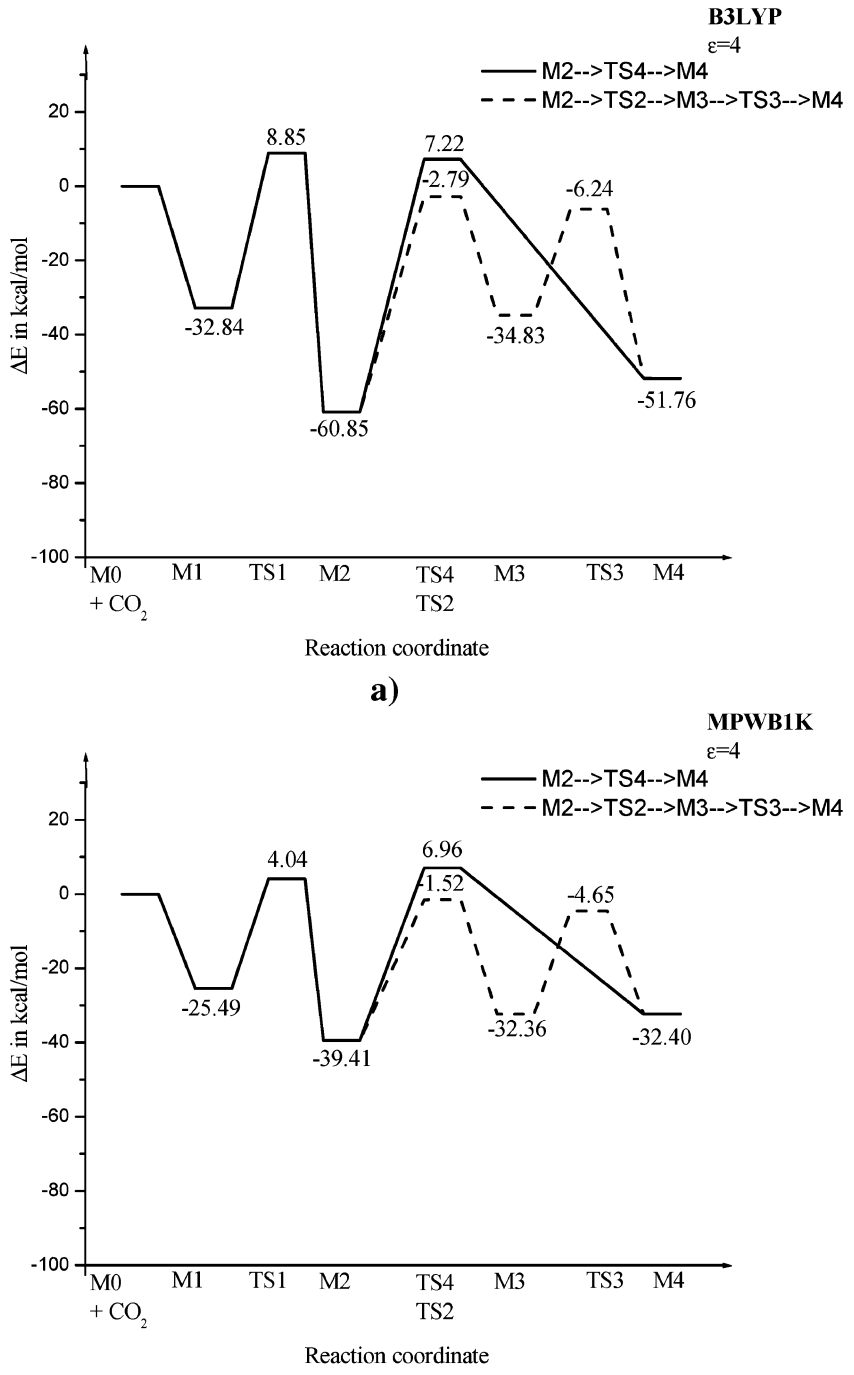

Figure 5. (a) B3LYP/DZVP and (b) MPWB1K/DZVP potential energy profiles for the Cd-CA in the protein environment (simulation with model B).

to the different manner with which the new functional treats the hydrogen bonds and all the present weak interactions. Such a type of interactions is of fundamental importance in biological systems and should be accurately described. In their work, Zao and Truhlar[81] said the MPWB1K functional gives good results especially for thermochemical kinetics and noncovalent interactions. In addition, they pointed out that only slight deterioration of reaction energies is generally observed with respect to the B3LYP or other older hybrid methods. Actually, the results on Cd-CA indicate that the MPWB1K barriers are sensibly lower as compared to B3LYP ones, but a significant difference is obtained between the B3LYP and MPWB1K reaction energy values (−87.21 vs −34.81 kcal/mol).

However, the MPWB1K functional does not introduce significant news about the followed mechanism in the sense that the determining step remains in overcoming the TS4 barrier.

Nevertheless, the strong lowering of both TS1 and TS4 (of 18.17 and 35.78 kcal/mol, respectively) in the MPWB1K computations matches better with the experimental observation concerning the proven activity of Cd-CA.[94]

Further tests on transition metal containing enzymes and comparisons with experimental counterparts are still necessary

to validate the MPWB1K functional and to establish if it works better than the most usual B3LYP in the description of such a type of systems.

Single-point estimation of the solvation energy, on the gas-phase B3LYP and MPWB1K equilibrium structures, was performed for Cd-CA enzyme. The dielectric constant of the continuum was taken to be 4. As indicated by Blomberg et al.[91] and by Noodleman et al.,[78] this value can effectively describe the combined effect of a protein embedded in a water solution on the solute.

Results are illustrated in Figure 5a (B3LYP) and b (MPWB1K).

The comparison between the two sets of data in solvent shows some difference with respect to the corresponding comparison in gas phase. The common aspects are the stabilization of all transition states and the minor exothermicity of the reaction in solvent. For intermediates, the situation cannot be generalized. In fact, M1, M2, and especially M4 appear to be less stable in solvent rather than in vacuo, at the B3LYP level. With the MPWB1K functional, the stabilization occurs for M1, M2, and M3.

Our data indicate that the interconversion barriers in the protein environment are lower than those found in gas phase, only at the B3LYP level. Thus, on the basis of computations with this functional, the catalytic process should be favored in solvent rather than in gas phase. In particular, the big barriers for going from M1 to M2 and from M2 to M4 result in being significantly reduced (decrease of 12.65 and of 9.87 kcal/mol, respectively). Instead, at the MPWB1K level, the reaction in solvent is faster as far as the M1 → TS1 → M2 and M3 → TS3 → M4 steps are concerned (interconversion barriers are 6.64 and 5.32 kcal/mol lower than in vacuo) but becomes slower in the M2 → TS4 → M4 and M2 → TS2 → M3 transformations (interconversion barriers are 4.21 and 2.20 kcal/mol higher than in vacuo).

Finally, both sets of calculations indicate the stability inversion of Lindskog (M2) and Lipscomb (M4) intermediates with respect to the gas phase.

In a previous work of Brauer et al.[65] on Zn-CA, the inclusion of water ($\epsilon = 80$) effects makes the M2 and M4 species almost isoenergetic. Bottoni et al.,[70] with the same formalism (COSMO) and a different dielectric constant ($\epsilon = 38.2$ nitromethane) continue to have the Lindskog intermediate significantly more stable than the Lipscomb one.

The behavior of Cd-CA in solvent appears to be different with respect to that of Zn-CA. In fact, no substantial differences in the energetics of the Zn-CA catalytic cycle, in going from gas to condensed phase, were found.[70] Nevertheless, since as mentioned before, the computations of Bottoni et al.[70] were performed in a different dielectric and with an approach different from ours, at the present time it is not appropriate to do a more detailed comparison.

Conclusions

Density functional B3LYP computations were carried out to explore the effect of the substitution of the zinc ion with cadmium in the carbonic anhydrase enzyme. The study was performed using two models to simulate the active site and two different strategies in order to alleviate the computational efforts in the case of the biggest model.

Computations on the advanced model were redone with a second-generation MPWB1K functional and introducing the effects of the protein environment.

The main results can be summarized as follows:

(1) The mechanism of the catalytic cycle depends strongly on the choice of the model used to simulate the active site of the enzyme. The indications obtained with the smallest model are in conflict with the experimental observation that suggests for cadmium a sensibly reduced activity with respect to the zinc-containing system. The addition of amino acidic residues Glu106 and Thr199, and a deep water molecule to the first model, reverses the previous conclusions, pointing the attention onto the importance that these residues have in ensuring a stabilizing network of hydrogen bonds around the active site.

(2) The different coordination chemistries due to the increasing size in going from zinc to the cadmium cation, and mainly the minor Lewis acid character of the second metal center, are responsible for the consistent stabilization of the intermediate M1 that represents the bottleneck for the cadmium reaction path. In particular, the strong σ bond that the CO_2 substrate forms with the −OH group opportunely activated by the cadmium ion, at M1 intermediate level, results in it being very difficult to be broken in the course of the catalytic cycle.

(3) Results with the MPWB1K functional indicate a path kinetically easier than that obtained at the B3LYP level owing to the lowering of the most significant barriers.

(4) The inclusion of the solvent effects causes a stability inversion of Lindskog and Lipscomb intermediates at both levels of theory. On the basis of the B3LYP description, the whole catalytic cycle proceeds more quickly in the protein environment rather than in gas phase, because of the reduction of the barrier heights. Only some steps of the reaction are kinetically favored in solvent, if the MPWB1K approach is followed. In particular, the result obtained with both functionals, concerning the decrease of the energy requirement for the M1−TS1−M2 transformation, becomes interesting in view of the effective working of the Cd−CA enzyme as suggested experimentally.

(5) The "inhibitory" effect of the cadmium on the catalytic activity of the carbonic anhydrase has a substantially kinetic nature being the thermodynamic aspect favorable to the substitution of zinc with the cadmium cation.

Acknowledgment. We gratefully acknowledge the University of Calabria and MIUR (MEMOBIOMAR project) for financial support.

Supporting Information Available: Full optimized geometrical parameters of the intermediates and transition states encountered in the Cd- and Zn-CA energy profiles using the model A. Cartesian coordinates (Å) for the various critical points located at B3LYP/DZVP level for model B. Atomic net charges for the species encountered in the Cd- and Zn-CA energy profiles using the model A. This material is available free of charge via the Internet at http://pubs.acs.org.

JA045546Q